2009 IEEE International Conference on Robotics and Automation
Kobe International Conference Center
Kobe, Japan, May 12-17, 2009

Loop-shaping H_∞-control of a 2-DOF piezoelectric-stack actuated platform for nanoscale positioning

Sumeet S. Aphale, Antoine Ferreira and S. O. Reza Moheimani

***Abstract*—Piezoelectric-stack actuated platforms are utilized in many nanopositioning applications. Their performance is limited by their low-frequency resonance due to the mechanical construction as well as piezoelectric nonlinear effects. We propose a hybrid control scheme comprising a loop-shaping H_∞ controller and an inversion-based feedforward control scheme, capable of delivering accurate nanopositioning performance at relatively high speeds, upto 40 Hz. It is shown that the implemented control strategy is robust in the presence of uncertainty in resonance frequency due to loading. It is also shown that by employing charge actuation on the fast axis and integral tracking control on the slow axis, accurate raster scans can be obtained. Experimental results that show resonance damping, integral tracking action as well as the robustness of the implemented control scheme to resonance frequency uncertainty are presented. Finally, raster scans recorded at 10 Hz, 20 Hz and 40 Hz are presented to show the achievable positioning performance.**

I. Introduction

To meet massively parallel production schedules in a variety of microsystem related applications such as three-dimensional nanometer-scale lithography, [1], $in-situ$ integrated circuit chip scanning [2], and high-speed wafer-level IC testing [3]; high performance nanopositioning stages are being investigated extensively. The scanning requirements imposed by larger-diameter 8" wafers present new challenges to designers of probe stations since stringent position control over a relatively large region (from micrometers to centimeters) with nanometer resolution and broad frequency range (Hz-kHz) are necessary [4]. Furthermore, as IC chips are continuously shrinking in size and the number of electrode pads is increasing (more than 2000 pads), overall prober positioning accuracy, repeatability and dynamics become difficult to sustain over temperature and time [5], [6]. Simple and robust construction, low cross-coupling between the axes and substantially large motion ranges have made the piezoelectric-stack actuated nanopositioning platforms quite popular in automatic probe testers of wafers. However, as the $x-y$ stage operates over a relatively large region (micro to millimeters) and in a broad frequency range (Hz-kHz), piezoactuators exhibit nonlinearities, system uncertainties and rate-dependent hysteresis which requires robust control designs that can effectively accommodate such behaviors.

In recent years, many open- and closed-loop control strategies capable of increasing the tracking precision and bandwidth of nanopositioning platforms have been proposed. Numerous nano-scale positioning techniques have also been documented in the past. In [7], robust tracking was reported. H_∞ control algorithms for nano-scale tracking have also been investigated [8]. Force-feedback for nanomanipulation was reported in [9]. Inversion-based feedforward techniques for continuously tracking a desired trajectory have been under investigation [10]. Inversion-based feedforward technique has also been applied to nanopositioning systems [11]. It was shown that by using this approach, it is possible to compensate for nonlinear effects such as creep and hysteresis [12]. High sensitivity to modeling errors and plant parameter uncertainties are the main drawbacks of the feedforward control strategy. Feedback techniques that suppress the effects of uncertainties have been shown to improve the bandwidth of feedforward strategies [13]. An in-depth overview of this field is given in [14].

Changes in resonance frequency is a commonly occurring system uncertainty in a nanopositioning stage. These variations can occur due to change in ambient temperature, humidity, atmospheric pressure and mechanical loading. Damping the structural resonance is the most effective method to make the system less sensitive to variations in resonance frequency. Passive damping techniques such as shunts have been effective but need constant tuning and show a drastic performance degradation under variations in resonance frequencies. Adaptive shunts are needed to cope with system uncertainties and have been reported in [15], [16]. Feedback controllers that impart substantial damping to the system have been documented over the years [17], [18]. PPF control [19] and Resonant control [20] have shown substantial damping capability. A straightforward control design approach is that of a polynomial-based controller [21]. This controller is easy to construct for second-order plants, imparts substantial damping to the system, and is robust under resonance frequency variations [22]. Combining such damping controllers that are insensitive to variations in resonance frequencies with a PI controller has been reported earlier [23], where it was noted that the high gain needed by the integrator to track a given trajectory limits the achievable scan speed using this technique to about 4 Hz.

A. Objectives

This work focuses on improving the scan performance of an industry-grade two degree-of-freedom (2-DOF) piezoelectric-stack actuated nanopositioning platform at relatively high frequencies. In this paper, we combine the loop-shaping H_∞ controller (LSC) design [24], [8], with the inversion-based feedforward technique [25]. We propose an integrated control design approach that achieves robustness and performance

Dr. Sumeet S. Aphale is a Research Fellow at the Center for Applied Dynamics Research (CADR), School of Engineering, Kings College, University of Aberdeen, UK

Prof. Antoine Ferreira [Corresponding author (antoine.ferreira@ensi-bourges.fr)] is with the PRISME Institute, University of Orléans, ENSIB 88 Boulevard Lahitolle, 18000 Bourges, France

Prof. S. O. Reza Moheimani is with the School of Electrical Engg. and Computer Sci. at the University of Newcastle, Callaghan, NSW, Australia

978-1-4244-2789-5/09/$25.00 ©2009 IEEE

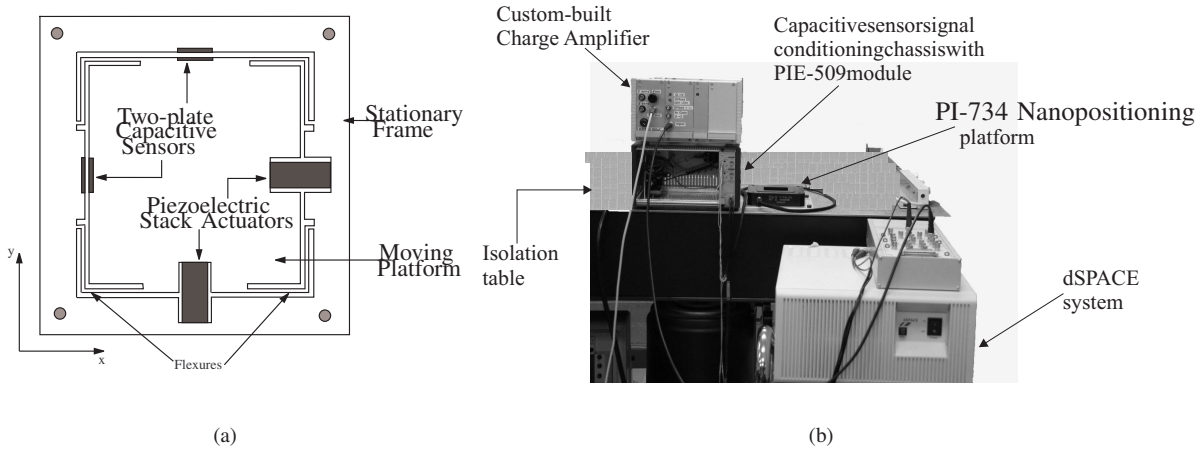

(a) (b)

Fig. 1. (a) Working principle of the monolithic XY piezoelectric-stack actuated nanopositioning platform.(b) A snapshot of the experimental setup used in this work

specifications that the aforementioned individual designs cannot achieve. Compared to [8], the proposed loop-shaping H_∞ controller permits important margins of parametric uncertainty and unmodeled dynamics at larger bandwidth frequencies. The loop-shaping H_∞ controller increases plant insensitivity to changes in resonance frequency by damping the resonance and thus, when combined with the inversion-based feedforward technique achieves a much larger positioning bandwidth with improved tracking accuracy. Piezoelectric stacks are prone to hysteresis errors that can be minimized by up to 89%, with the use of charge amplifiers, [26]. A custom-built charge amplifier capable of driving the typically high capacitive loads presented by the piezoelectric stacks ($\approx 10\ \mu$F) is used to drive the piezoelectric stack actuators, thus improving the tracking performance.

B. Organization

Description of the experimental setup used in this work as well as the system identification is given in Section II. Section III will give details of the implemented control strategy. Experimental closed-loop and raster scanning results will be presented in Section IV to show the improvement in scan performance due to feedback and inversion-based feedforward. Section V concludes the article.

II. 2-DOF Piezoelectric Nanopositioning Platform: Brief Description and System Identification

The PI-734 nanopositioning platform, used in this work, is a two-axis piezoelectric stack-actuated platform based on a parallel-kinematic design. This design provides mounting independent orthogonality and reduced cross-coupling between the two axes. Friction and stiction are eliminated by using a flexure guidance system. To increase the range of motion whilst maintaining the sub-nanometer accuracy of the platform, it is equipped with a built-in integrated lever motion amplifier. Each axis of the nanopositioning platform is fitted with a two-plate capacitive sensor that provides a direct position measurement. A simplified diagram of the nanopositioning platform is given in Figure 1 (a). The piezoelectric stack actuators take voltage input in the range of 0 V - 100 V for each axis. The resultant motion produced by the platform is within 0 μm - 100 μm. This motion is detected by the two-plate capacitive sensors and fed to an electronic sensor output module. The output of this module is within 0 V - 6.7 V.

A. System Identification

A dSPACE-1005 rapid prototyping system equipped with 16-bit ADC(DS2001) and DAC(DS2102) cards with a sampling frequency of 20 kHz, is used to implement the proposed strategy. The fast axis is charge-actuated by means of an in-house, custom built charge amplifier with an equivalent voltage gain of 21. The slower axis was driven using an inverting voltage amplifier with a voltage gain of 20. The frequency response of each axis from input voltage (or charge) to output displacement (in terms of capacitive sensor voltage) was recorded using a HP signal analyzer. Throughout this work, the piezoelectric stack actuator was kept at a bias of +40 V, to avoid depolarization due to application of negative voltages. As the identification was done from 10 Hz onwards, the effect of creep was eliminated due to the absence of any low-frequency components. The piezoelectric stack on the other axis was shorted out to eliminate cross-coupling effects during system identification. The output displacement (d in μm) is obtained by scaling the measured capacitive sensor voltages by the proportional scaling factor ($0.067\ V/\mu m$). A picture of the complete setup is given in Figure 1(b).

The first resonance for one axis occurs at 426 Hz and at 395 Hz for the other axis. A periodic trianglular signal and a staircase type waveform are used to generate a raster scan. Based on achievable bandwidth considerations, it is beneficial to drive the axis with the higher resonance frequency by a triangular waveform and the axis with the lower resonance frequency by the staircase waveform. Throughout this paper, the axis with its resonance at 426 Hz will be known as the *fast axis* while the axis with its first resonance at 395 Hz

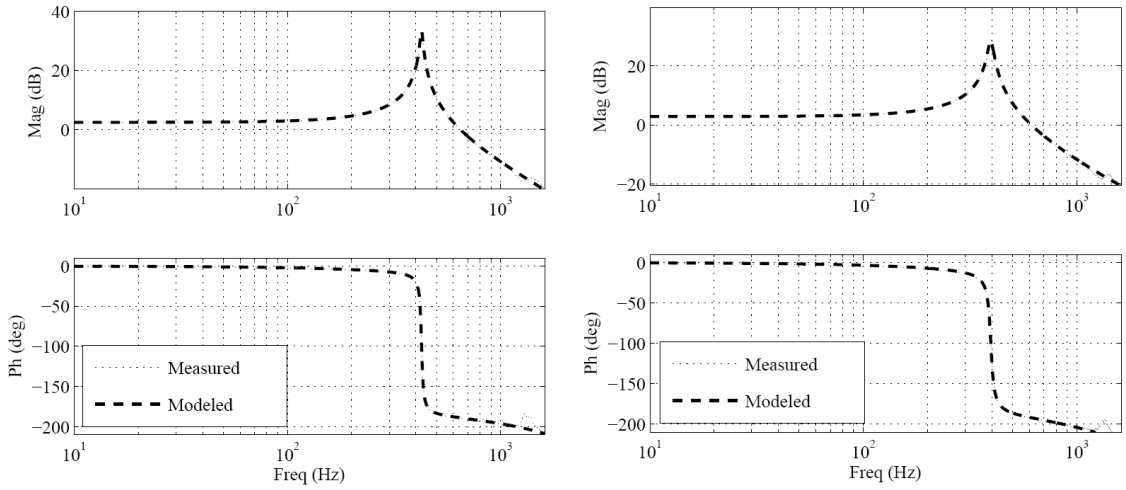

Fig. 2. Frequency response plots for the measured and modeled X (a) and Y (b) axes of the nanopositioning platform

will be deemed the *slow axis*. A subspace-based modeling technique, [27], is used to obtain accurate models of the open-loop system. Figure 2 shows the measured frequency response of the open-loop system. A subspace-based second-order model accurately captures the system dynamics in the bandwidth of interest and is used throughout this work for further analysis and computations.

III. Control Design and Implementation

The implemented control scheme is shown in Fig.3. The mode of operation of the nanopositioning platform is such that higher bandwidth requirements are made on *x*-stage whereas the *y*-stage is made to move relatively slowly in order to cope with high-speed wafer-level IC testing. In the control technique design presented in Fig.3, both the controllers *LSC* and K_∞ are based on a robust loop-shaping H_∞-controller. The latter increases plant insensitivity to changes in resonance frequency and thus, when combined with the inversion-based feedforward technique achieves a much larger positioning bandwidth with improved tracking accuracy. *I* stands for an integral tracking controller with a suitably high gain.

A loop-shaping controller is designed based on the McFarlane-Glover design procedure [24]. This technique incorporates loop shaping methods to obtain performance/robust stability tradeoffs by solving a H_∞ optimization problem at all frequencies of interest. The model uncertainties are included as perturbations to the nominal plant model, and robustness is guarateed by ensuring that the stability is satisfied for the worst-case uncertainty. The loop-shaping weights W_1 and W_2 are stable minimum-phase LTI weighting functions. These pre- and post-compensator weighting functions are selected such that the gain of the 'shaped plant', $G_s = W_2 G W_1$, is sufficiently high at frequencies where good disturbance attenuation is required and is sufficiently low at frequencies where good robust stability is required. The idea is to generate a controller K_s that robustly stabilizes a family of systems given by a ball

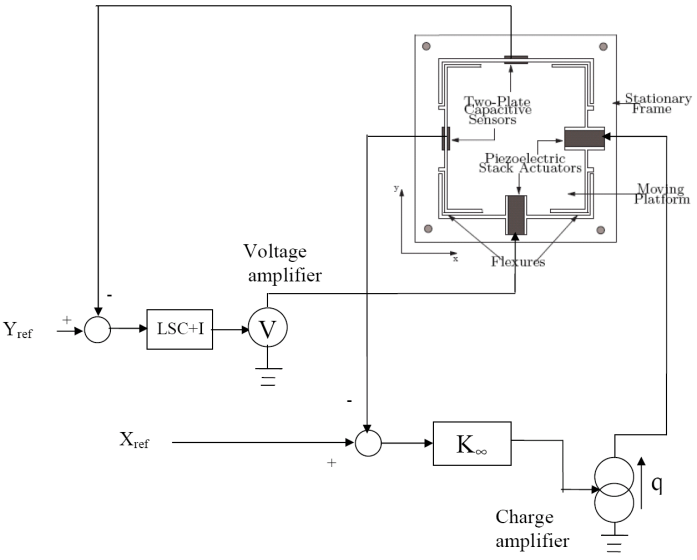

Fig. 3. A schematic of the implemented overall control strategy. The fast axis is actuated using a charge amplifier while the slow axis is actuated using a voltage amplifier. To reduce the nonlinear effects of hysteresis and improve tracking in the voltage actuated slow axis, an integral controller is implemented along with a loop-shaping controller used for resonance damping.

of uncertainty in the normalized coprime factors of the shaped plant G_s.

As our plant is a SISO system, we can simply assign $W_1 = 0.5$ and put the main emphasis on the choice of W_2. As the plant has been identified over a limited bandwidth (10 Hz - 1.61 kHz), the high-frequency dynamics are unknown and may cause closed-loop instabilities. Control of these high-frequency dynamics deems the plant less prone to instability due to accidental excitation of these unidentified dynamics.

The post-compensator is chosen such that with

$$W_2 = \frac{5.053 \times 10^7}{s^2 + 4021s + 2.527 \times 10^7}, \quad (1)$$

the shaped plant, G_s, has low gain at D.C. and at low frequencies while its higher frequency dynamics roll-off at a faster rate. These weights are used to synthesize the H_∞-based controller K_s that robustly stabilizes the shaped plant G_s. Using the command "*ncfsyn*" from the MATLAB μ-Analysis and Synthesis Toolbox, the robust controller,

$$K_s = \frac{-2.358s^3 - 5735s^2 - 4.307 \times 10^7 s + 1.021 \times 10^{11}}{s^3 + 1.243 \times 10^4 s^2 + 9.15 \times 10^7 s + 4.13 \times 10^{11}} \quad (2)$$

was obtained. This controller also results in good gain and phase margins (G.M. = 10.3 dB at 872.17 Hz and P.M. = 68.8 deg at 552.26 Hz). The resulting loop shaping controller $K = W_1 K_s W_2$ is fifth order.

Using a similar approach, a loop-shaping controller was designed for the slow axis of the nanopositioning platforms. The details are given below.

$$W_1' = 0.45$$

$$W_2' = \frac{5.053 \times 10^7}{s^2 + 6032s + 2.527 \times 10^7}$$

$$K_s' = \frac{-2.417s^3 - 2400s^2 - 1.46 \times 10^7 s + 6.96 \times 10^{10}}{s^3 + 1.091 \times 10^4 s^2 + 6.442 \times 10^7 s + 2.385 \times 10^{11}}$$

This controller has good gain and phase margins (G.M. = 8.49 dB at 697 Hz and P.M. = 58.6 deg at 523 Hz) and also damps the resonant mode by 23 dB. To be able to track the pseudo-ramp waveform used to produce the required raster scan, a pure integrator with a gain of 600 is implemented in the outer loop. The combined system is stable and has good gain and phase margins as well (G.M. = 9.53 dB at 197 Hz and P.M. = 64.6 deg at 55.5 Hz).

A. Inversion-based Feedforward controller

Input-shaping using plant inversion is a well-known and popular technique for achieving accurate scan performance using nanopositioning devices. An inversion-based feedforward controller cannot achieve satisfactory tracking performance in the presence of plant uncertainties. Variations in resonance frequency and damping are two important uncertainties that can occur in nanopositioning platforms. In the presence of such uncertainties, the achievable positioning bandwidth of the platform is substantially degraded. In the proposed input-shaping method using plant inversion, the closed-loop plant, G_{cl}, is identified and inverted. The desired input, u_{ref}, is fed to this inverted plant model, $\widetilde{G}_{cl}^{-1}$, and this output, u_{inv}, is fed to the actual closed-loop plant, G_{cl}, to obtain the desired output y_{des}. Note that the closed-loop plant has been identified for a finite number of frequencies and thus errors due to higher unmodeled input harmonics are present but are very small. A pictorial representation of this scheme is given in Figure 4. For more details, the reader is reffered to [28].

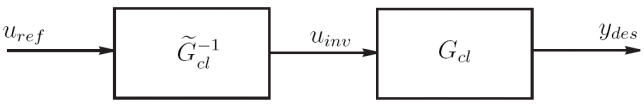

Fig. 4. Implemented inversion strategy for accurate tracking within the available bandwidth.

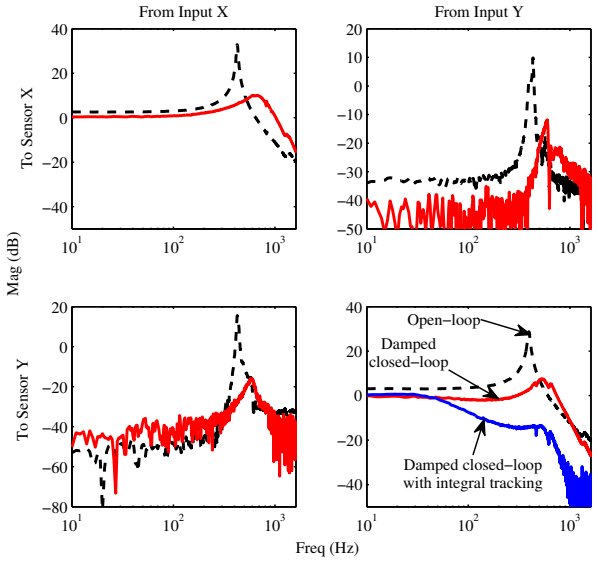

Fig. 5. The fast axis (X) has loop-shaping control. The slow axis (Y) has loop-shaping control and integral tracking. The fast axis is charge driven and thus the nonlinear effects of hysterisis are minimal. The slow axis is driven by voltage and the integral control is implemented to enforce tracking and reduce nonlinear effects. The closed-loop 3-dB bandwidth of the slow axis is 60 Hz.

IV. Experimental Results

Open- and closed-loop frequency responses of the system are plotted in Figure 5. It is clear that the cross-coupling is also reduced in closed-loop. It is also clear that tracking bandwidth of the slow axis is limited to 60 Hz due to the presence of the integral loop action. To check for robustness under variation in resonance frequency, the platform was loaded with a mass of 50 gm. This shifts the resonance by a substantial amount, from 426 Hz to 350 Hz. The implemented control strategy is capable of damping the resonant mode by more than 20 dB, even under the presence of resonance frequency uncertainties, 6.

Open and closed loop plots for 10 Hz, 20 Hz and 40 Hz triangular trajectories are recorded. These are plotted in Figure 7. The open- and closed-loop RMS errors are tabulated in Table I. The scan range is limited to 16 μm due to the current limit of the charge drive. As can be seen from Table I, the RMS error is maximum at 40 Hz and is equal to 0.24% of the total scan range (in closed-loop).

Raster scans were obtained by exciting the fast axis with a periodic triangle wave and the slow axis with a synchronized pseudo-ramp input signal. Raster scans were recorded at 10 Hz, 20 Hz and 40 Hz as shown in Figure 8. 15 μm wide scans were obtained with a line spacing of 72 nm. At 10 Hz, the

TABLE I
TABLE SHOWING THE RMS VALUE OF ERROR BETWEEN THE DESIRED AND MEASURED SCANS AT THREE FUNDAMENTAL FREQUENCIES.

Fundamental frequency for the triangular waveform (Hz)	Open-loop RMS error (nanometers)	Closed-loop RMS error (nanometers)
10	81.8	21.3
20	224.4	32.9
40	653.7	38.8

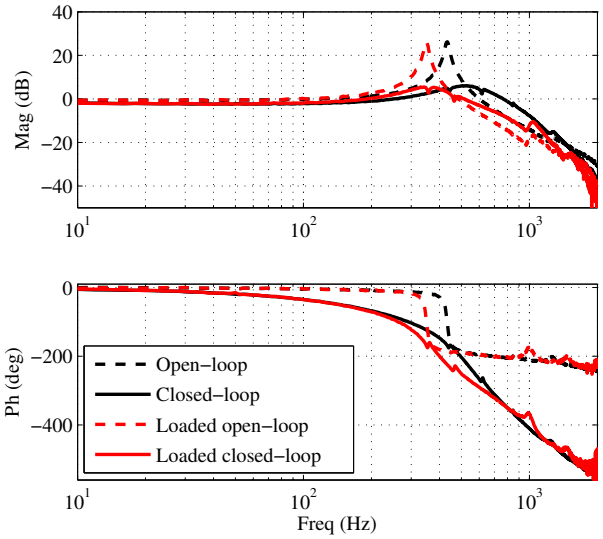

Fig. 6. Open- and closed-loop frequency responses of the nominal and the system loaded with a mass of 50 gm. As the loading inceases, the bandwidth of the closed-loop system reduces, but the resonance is damped and the system is stable.

scans have a full 15 μm linear range. At 20 Hz, the linear range drops to 80% of the full range and at 40 Hz, the linear range is greatly reduced to less than 55%. This is due to the tracking bandwidth limitation of the slow axis (3 dB at 60 Hz). The noise is predominantly quantization noise coupled with noise from the capacitive sensor and has an RMS value of about 13 nm.

V. CONCLUSIONS

A loop-shaping H_∞ controller with good stability margins that imparts 23 dB of damping to the dominant resonant mode of both the platform axes is designed. Additionally, it is shown to be robust in presence of resonance frequency uncertainties due variations in platform loading, with minimal degradation in positioning and damping performance. Triangle scans of up to 40 Hz were traced with high accuracy by the closed-loop controlled nanopositioning platform. The RMS error over all scan was as low as 0.24% at scan frequencies as high as 40 Hz. Due to the limited bandwidth offered by the high-gain integral tracking controller, linear scan ranges achievable were inversely proportional to the scan speeds, i.e., higher speeds resulted in lower linear scan ranges. Yet, 55% linear range was achieved at 40 Hz while 80% and 95% linear ranges were achieved at 20 Hz and 10 Hz respectively. This is quite an improvement from the 4 Hz scans obtained earlier with the same nanopositioner setup, making this strategy suitable for relatively high-speed applications.

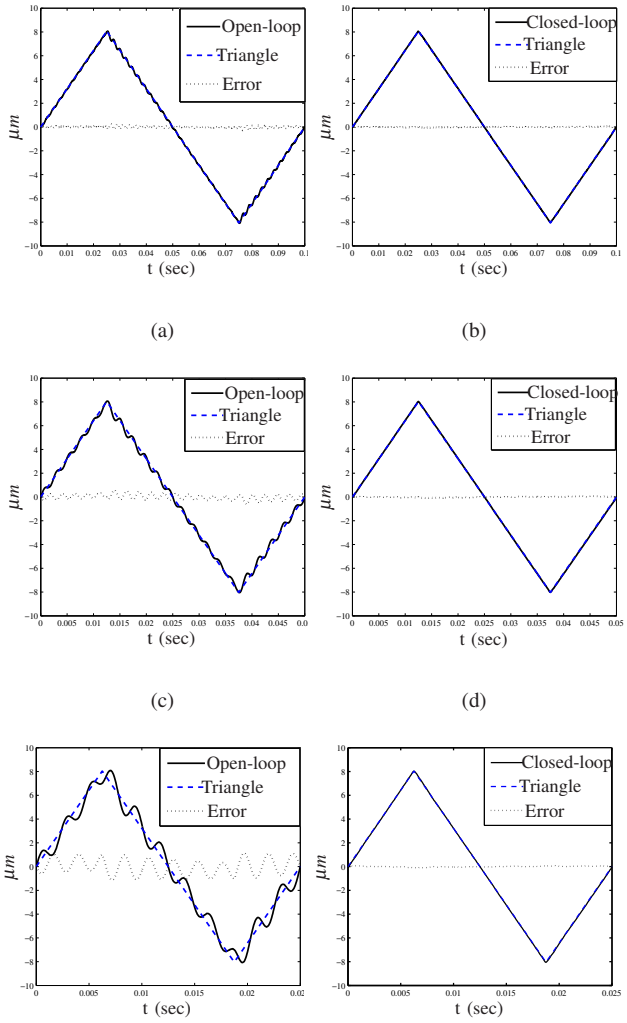

Fig. 7. (a),(c) and (d) show the open-loop (undamped) plots for 10 Hz, 20 Hz and 40 Hz triangular scan outputs respectively. (b), (d) and (f) show the closed-loop (feedback and inversion-based input shaping combined) tracking results for the same. Note that in closed-loop, the tracking is visibly superior. As the frequency content in the scan signal increases, the scan performance of the closed-loop worsens due to loss of bandwidth.

ACKNOWLEDGMENT

This research was supported by the Australian Research Council's Center of Excellence for Complex Dynamic Systems and Control.

REFERENCES

[1] S. Thian, Y. Tang, J. Fuh, Y. Wong, L. Lu, and H. Loh, "Micro-rapid-prototyping via multi-layered photo-lithography," *The Interna-*

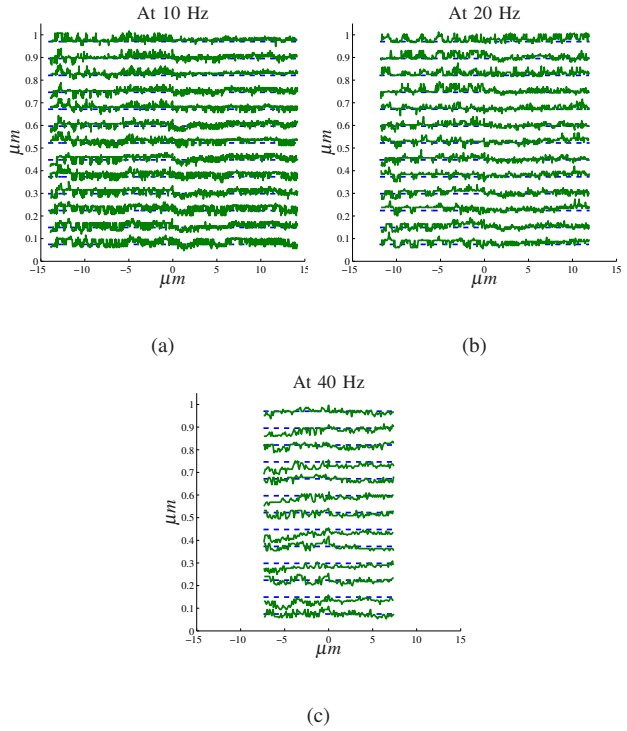

Fig. 8. Raster scans obtained at 10 Hz, 20 Hz and 40 Hz. The solid green line denotes the measured data while the dotted blue line is the reference.

tional Journal of Advanced Manufacturing Technology, vol. 29, no. 9 - 10, pp. 1026 – 1032, July 2006.

[2] V. Meister and K. Potje-Kamloth, "In situ control of the electrochemical gap height modification of a suspended gate field-effect transistor by capacitance-voltage measurement technique," *Sensors and Actuators B: Chemical*, vol. 46, no. 3, pp. 226 – 235, May 1998.

[3] B. Leslie and F. Matta, "Wafer-level testing with a membrane probe"," *IEEE Design and Test of Computers*, vol. 6, no. 1, pp. 10 – 17, 1989.

[4] G. Yang, J. A. Gaines, and B. J. Nelson, "A supervisory wafer-level 3D microassembly system for hybrid MEMS fabrication," *Journal of Intelligent and Robotic Systems*, vol. 37, no. 1, pp. 42 – 68, 2003.

[5] J. Geary and G. Vella-Coleiro, "Cryogenic wafer prober for josephson devices," *IEEE Transactions on Magnetics*, vol. 19, no. 3, pp. 1190–1192, 1989.

[6] M. G. Wassink, M. van de Walb, C. Scherera, and O. Bosgraa, "LPV control for a wafer stage: beyond the theoretical solution," *Control Engineering Practice*, vol. 13, no. 2, pp. 231–245, 2005.

[7] S. Salapaka, A. Sebastin, J. P. Cleveland, and M. V. Salapaka, "High bandwidth nano-positioner: A robust control approach," *Review of Scientific Instruments*, vol. 73, no. 9, p. 3232 3241, 2002.

[8] A. Sebastian and S. M. Salapaka, "Design methodologies for robust nano-positioning," *IEEE Transactions on Control Systems Technology*, vol. 13, no. 6, pp. 868 – 876, November 2005.

[9] M. Sitti and H. Hashimoto, "Teleoperated touch feedback from the surfaces at the nanoscale: Modeling and experiments," *IEEE/ASME Transactions on Mechatronics*, vol. 8, pp. 287 – 298, February 2003.

[10] M. Tomizuka, "On the design of digital tracking controllers," *ASME Journal of Dynamic Systems, Measurement and Control*, pp. 412 – 418, November 1993.

[11] Q. Zhou and S. Devasia, "Preview-based optimal inversion for output tracking: Application to scanning tunneling microscopy," *IEEE Transactions on Control Systems Technology*, vol. 12, no. 3, pp. 375 – 386, May 2004.

[12] D. Croft, G. Shedd, and S. Devasia, "Creep, hysteresis, and vibration compensation for. piezoactuators: Atomic force microscopy application," *Journal of Dynamic Systems, Measurement, and Control*, vol. 123, no. 1, pp. 35–43, March 2001.

[13] Y. Zhao and S. Jayasuriya, "Feedforward controllers and tracking accuracy in the presence of plant uncertainties," *Trans. of ASME, Journal of Dynamic Systems, Measurement and Control*, vol. 117, pp. 490 – 495, December 1995.

[14] S. Devasia, E. Eleftheriou, and S. O. R. Moheimani, "A survey of control issues in nanopositioning," *IEEE Transactions on Control Systems Technology*, vol. 15, no. 5, pp. 802–823, September 2007.

[15] A. J. Fleming and S. O. R. Moheimani, "Adaptive piezoelectric shunt damping," *IEEE Transactions on Control Systems Technology*, vol. 12, pp. 18 – 28, February 2003.

[16] D. Niederberger, A. J. Fleming, S. O. R. Moheimani, and M. Morari, "Adaptive multimode resonant piezoelectric shunt damping," *IEEE Transactions on Control Systems Technology*, vol. 18, no. 2, pp. 291–315, October 2004.

[17] B. Kang and J. K. Mills, "Vibration control of a planar parallel manipulator using piezoelectric actuators," *Journal of Intelligent and Robotic Systems.*, vol. 42, no. 1, pp. 51–70, 2005.

[18] T. Ando, N. Kodera, D. Maruyama, E. Takai, K. Saito, and A. Toda, "A high-speed atomic force microscope for studying biological macromolecules in action," *Japanese Journal of Applied Physics*, vol. 41, no. 7B, pp. 4851–4856, 2002.

[19] J. L. Fanson and T. K. Caughey, "Positive position feedback control for large space structures," *AIAA Journal*, vol. 28, no. 4, pp. 717 – 724, 1990.

[20] H. R. Pota, S. O. R. Moheimani, and M. Smith, "Resonant controllers for smart structures," *IEEE Transactions on Control Systems Technology*, vol. 11, no. 1, pp. 1 – 8, 2002.

[21] G. C. Goodwin, S.F. Graebe and M. E. Salgado, *Control System Design*. Prentice Hall International, Inc, 2001.

[22] B. Bhikkaji, M. Ratnam, A. J. Fleming, and S. O. R. Moheimani, "High-performance control of piezoelectric tube scanners." *IEEE Transactions on Control Systems Technology*, vol. 5, no. 5, pp. 853 – 866, September 2007.

[23] S. S. Aphale, B. Bhikkaji, and S. O. R. Moheimani, "Minimizing scanning errors in piezoelectric stack-actuated nanopositioning platforms," *IEEE Transactions on Nanotechnology*, vol. 7, no. 9, pp. 79 – 90, 2008.

[24] D. McFarlane and K. Glover, "A loop shaping design procedure using synthesis," *IEEE Transactions on Automatic Control*, vol. 37, no. 6, pp. 759 – 769, June 1992.

[25] T. Tsao, "Optimal feedforward digital tracking controller design," *ASME Journal of Dynamic Systems, Measurement and Control*, vol. 116, no. 4, pp. 583 – 592, December 1994.

[26] A. Fleming and S. O. R. Moheimani, "A ground-loaded charge amplifier for reducing hysteresis in piezoelectric tube scanners," *Review of Scientific Instruments*, vol. 76, no. 7, 2005.

[27] T. McKelvey, H. Akcay, and L. Ljung, "Subspace based multivariable system identification from frequency response data," *IEEE Transactions on Automatic Control*, vol. 41, no. 7, pp. 960–978, July 1996.

[28] S. S. Aphale, S. Devasia, and S. O. R. Moheimani, "High-bandwidth control of a piezoelectric nanopositioning stage in the presence of plant uncertainties," *Nanotechnology*, vol. 19, p. 125503 (9pp), 2008.